Contribution to the study of cylindrical adhesive joining

O. Nemeş[a,*], F. Lachaud[b,**], A. Mojtabi[c]

[a]*UTC-N, Facultatea de Ştiinţa şi Ingineria Materialelor, B-dul Muncii nr. 103-105, 400641, Cluj-Napoca, Romania*
[b]*ENSICA, Département Génie Mécanique, 1 place Émile Blouin, 31056 Toulouse cedex 5, France*
[c]*IMFT, UPS Toulouse III, UFR-MIG, 118 route de Narbonne, 31062 Toulouse cedex 4, France*

Abstract

This paper presents a study of the stress analysis in cylindrical assemblies. For the present study we use a cylindrical assembly of two tubes. We write all the components of the stress field function of the $\sigma_{zz}^{(1)}(z)$ stress in the first tube and then we introduce these components into the potential energy formulation. Our method is a variational method applied on the potential energy of deformation. The model can predict the intensity and the distributions of stresses in the assembly. We can also analyse the influence of some geometrical or material parameters on the stress field.

Keywords: C. Stress analysis; C. Stress distribution; E. Joint design; Metals

1. Introduction

The increase in the use of adhesive bonded joints is due to the many advantages of this method compared to traditional methods. This assembling method distributes stresses over the whole joining surface and removes the concentrations of stresses to the boundary of holes generated by bolting or riveting assemblies. Another factor in the increased use of adhesive bonded joints is the appearance of composite materials, because their mechanical performances decrease if the assembly requires machining.

The mechanical performance of an adhesive bonded joint is related to the distribution of stresses in the adhesive layer. Consequently it is essential to know this distribution, which, because of its complexity, makes the prediction of fractures difficult. From the first works of Volkersen [1], which give only a distribution of the shear stress in the adhesive joint, to the more recent studies by finite elements, many formulations have made it possible to define the field of stresses in such assemblies in a better way.

Compared to the number of recent scientific publications concerning plane joints, with single or double lap [2–9], there are only a few theoretical works concerning the study of mechanical behaviour in adhesive assemblies with symmetry of revolution under tensile loading [10–14], subjected to torsion [15] or a harmonic axial load [16].

Lubkin and Reissner [17] present an analysis of stresses in tubular assemblies subjected to an axial loading and give a solution of the peeling stress distribution in the thickness of the adhesive. The tubes are supposed to be of small thickness, and they use the theory of thin walls to build the stress field. Their analysis assumes that the work of shear and peel stresses in the two tubes is negligible relative to that of the same stresses in the adhesive.

Alwar and Nagaraja [18] made a study by finite elements of tubular joining subjected to an axial load, taking into account the viscoelastic behaviour of the adhesive. They also showed that the viscoelastic behaviour of the adhesive makes it possible to predict a considerable reduction in the maximum stresses at the ends of the joint.

Other more recent work confronts experimental results with analytical computation results from the classical theory, to which are added correcting fields. Others draw

*Corresponding author. Fax: +40 (0)264 41 51 54.
**Corresponding author. Fax: +33 (0)5 61 61 85 95.
E-mail addresses: Ovidiu.Nemes@sim.utcluj.ro (O. Nemeş), Frederic.Lachaud@ensica.fr (F. Lachaud).

a certain number of conclusions on optimisation of the various geometrical and structural parameters, conferring maximum mechanical strength on the assembly when it is under tensile loading.

The most recent work concerning the type of assembly considered is by Shi and Cheng [11]. They build a first stress field using equilibrium equations and the conditions of continuity of stresses at the interfaces using an equation of compatibility. They then calculate the potential energy associated with this field, and, using the theorem of minimal complementary energy, obtain a system of differential equations, the solutions of which are used to determine the optimal field.

2. Theoretical model

All work has encountered difficulties in modelling the stress field in the vicinity of the ends of the joint. The method used to obtain the optimal field for this type of assembly consists of:

- construction of a statically acceptable field,
- calculation of the potential energy associated with the stress field,
- minimisation of this energy by the variational method, and
- resolution of the differential equation obtained.

2.1. Geometrical definitions and hypothesis

In this study we consider an assembly of tubes subjected to a tensile load whose geometrical definitions are represented in Fig. 1, where we have the following notations: E_c, v_c, Young's modulus and Poisson's ratio of the adhesive ©; E_{tl}, E_{ll}, v_{tll}, longitudinal, transverse modulus and Poisson's ratio of the inner tube; E_{2t}, E_{2l}, v_{tl2}, longitudinal, transverse modulus and Poisson's ratio of the external tube; r_i, internal radius of the inner tube; r_{ic}, external radius of the inner tube; r_{ec}, internal radius of the external tube; r_e, external radius of the external tube; L, joining length; and f and q, tensile stresses following along the z-axis, on the inner and outer tubes, respectively.

The constraints in various materials will be referenced by the index (i) ($i = ①$—the internal tube, ©—the adhesive and ②—the external tube).

To build the statically acceptable field, we adopt the following assumptions:

- The radial stress $\sigma_{rr}^{(i)} = 0$ is null in the three domains.
- The revolution symmetry imposes that the shear stress is null:

$$\tau_{r\theta} = \tau_{z\theta} = 0. \tag{1}$$

- The stress in the adhesive will be neglected:

$$\sigma_{zz}^{(©)} = 0. \tag{2}$$

- The axial stress will be a function of only "axial" variable z.

The constraint field is reduced to the following components:

- Inner tube (①):

$$\sigma_{zz}^{(1)}(z), \quad \tau_{rz}^{(1)}(r,z), \quad \sigma_{\theta\theta}^{(1)}(r,z). \tag{3}$$

- Adhesive (©):

$$\sigma_{\theta\theta}^{(©)}(r,z), \quad \tau_{rz}^{(©)}(r,z). \tag{4}$$

- Outer tube (②):

$$\sigma_{zz}^{(2)}(z), \quad \tau_{rz}^{(2)}(r,z), \quad \sigma_{\theta\theta}^{(2)}(r,z). \tag{5}$$

By introducing the adopted assumptions, the equilibrium equations in cylindrical co-ordinates are reduced to the

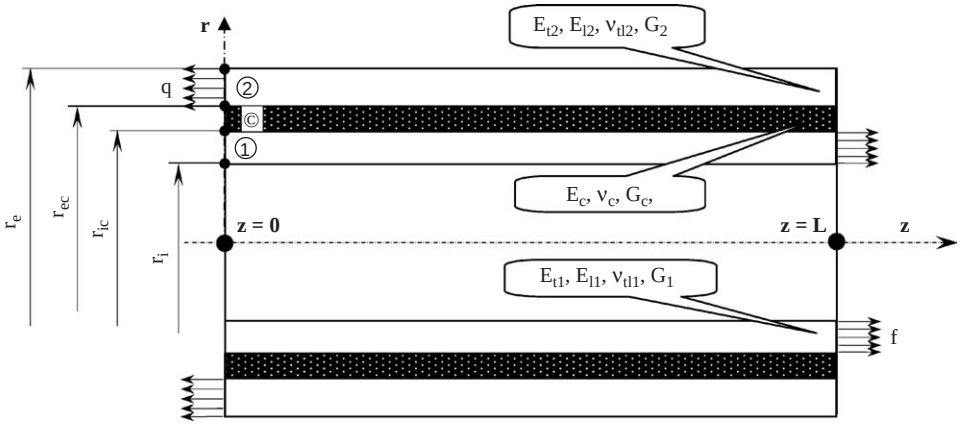

Fig. 1. Geometrical and material definitions of the assembly.

following two expressions:

$$-\frac{1}{r}\sigma_{\theta\theta}+\frac{\partial\tau_{rz}}{\partial z}=0, \tag{6}$$

$$\frac{\partial\tau_{rz}}{\partial r}+\frac{1}{r}\tau_{rz}+\frac{\partial\sigma_{zz}}{\partial z}=0. \tag{7}$$

By writing the equilibrium of the assembly we obtain the relation that connects the two loads f and q with the $\sigma_{zz}^{(i)}(z)$ stresses:

$$\left(r_{\mathrm{ic}}^2-r_{\mathrm{i}}^2\right)\sigma_{zz}^{(1)}+\underbrace{\left(r_{\mathrm{ec}}^2-r_{\mathrm{ic}}^2\right)\sigma_{zz}^{(C)}}_{0}+\left(r_{\mathrm{e}}^2-r_{\mathrm{ec}}^2\right)\sigma_{zz}^{(2)} = \left(r_{\mathrm{ic}}^2-r_{\mathrm{i}}^2\right)f=\left(r_{\mathrm{e}}^2-r_{\mathrm{ec}}^2\right)q. \tag{8}$$

2.2. Stress field definition

For the inner tube (①):

By writing the equilibrium of an elementary length section of tube (Fig. 2) we are able to express the shear stress $\tau_{rz}^{(1)}$:

$$\tau_{rz}^{(1)}(r,z)=\frac{\left(r_i^2-r^2\right)}{2r}\frac{\mathrm{d}\sigma_{zz}^{(1)}}{\mathrm{d}z}. \tag{9}$$

From expression (9) and equilibrium equation (6), we express directly the orthoradial stress in the material ①:

$$\sigma_{\theta\theta}^{(1)}(r,z)=\frac{\left(r_{\mathrm{i}}^2-r^2\right)}{2}\frac{\mathrm{d}^2\sigma_{zz}^{(1)}}{\mathrm{d}z^2}. \tag{10}$$

For the adhesive Ⓒ:

With the help of Eq. (7) and the continuity condition of the shear stress for $r=r_{\mathrm{ic}}$, we obtain the expression for the shear stress $\tau_{rz}^{(c)}$:

$$\tau_{rz}^{(c)}(r,z)=\frac{\left(r_{\mathrm{i}}^2-r_{\mathrm{ic}}^2\right)}{2r}\frac{\mathrm{d}\sigma_{zz}^{(1)}}{\mathrm{d}z}. \tag{11}$$

The expression of the orthoradial stress in the adhesive is obtained as for the inner tube ①:

$$\sigma_{\theta\theta}^{(c)}(r,z)=\frac{\left(r_{\mathrm{i}}^2-r_{\mathrm{ic}}^2\right)}{2}\frac{\mathrm{d}^2\sigma_{zz}^{(1)}}{\mathrm{d}z^2}. \tag{12}$$

For the outer tube (②):

The expression for shear stress in the external tube can be given in two ways: either by considering the balance of a section of tube or by using the equilibrium equation (7) and the condition of continuity of this same constraint at the interface with the adhesive. These two methods lead to the same expression:

$$\tau_{rz}^{(2)}(r,z)=\frac{\left(r_{\mathrm{e}}^2-r^2\right)\left(r_{\mathrm{ic}}^2-r_{\mathrm{i}}^2\right)}{2r\left(r_{\mathrm{ec}}^2-r_{\mathrm{e}}^2\right)}\frac{\mathrm{d}\sigma_{zz}^{(1)}}{\mathrm{d}z}. \tag{13}$$

The orthoradial stress is obtained immediately:

$$\sigma_{\theta\theta}^{(2)}(r,z)=\frac{\left(r_{\mathrm{e}}^2-r^2\right)\left(r_{\mathrm{ic}}^2-r_{\mathrm{i}}^2\right)}{2r\left(r_{\mathrm{ec}}^2-r_{\mathrm{e}}^2\right)}\frac{\mathrm{d}^2\sigma_{z}^{(1)}}{\mathrm{d}z^2}. \tag{14}$$

The orthoradial stress in the adhesive is independent of r. This is due to the nullity of the $\sigma_{zz}^{(c)}(z)$ stress. We can see that the orthoradial stress is continuous over interfaces with the adhesive. This continuity results from the starting hypothesis in which we consider the radial stress as null.

Now the field is entirely determined and its components are written according to the stress in the inner tube $\sigma_{zz}^{(1)}$.

For the rest of the problem we must use the boundary conditions, those that translate the presence of edges into $z=0$ and $z=L$.

$$\begin{aligned} &z=0;\ \sigma_{zz}^{(1)}(0)=q;\ \tau_{rz}^{(c)}(r,0)=0;\\ &z=L;\ \sigma_{zz}^{(1)}(L)=0;\ \tau_{rz}^{(c)}(r,L)=0. \end{aligned} \tag{15}$$

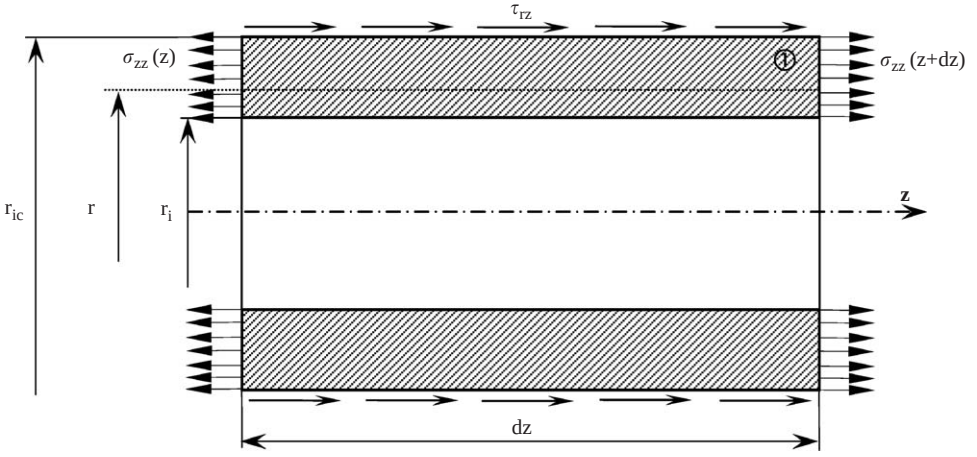

Fig. 2. Equilibrium of an elementary length section of the inner tube, $r\in[r_{\mathrm{i}},\ r_{\mathrm{ic}}]$.

2.3. Expression of potential energy

Because the tubes considered are transversally isotropic and the adhesive isotropic, the potential energy can be written as

$$\xi_p = \pi \int_0^L \int_{r_i}^{r_{ic}} \left[\frac{\sigma_{\theta\theta}^{(1)2}}{E_{1t}} + \frac{\sigma_{zz}^{(1)2}}{E_{1l}} - \frac{2\nu_{tl1}}{E_{1t}} \sigma_{zz}^{(1)} \sigma_{\theta\theta}^{(1)} + \frac{1}{G_1} \tau_{rz}^{(1)2} \right] r \, dr \, dz + \pi \int_0^L \int_{r_{ic}}^{r_{ec}} \frac{1}{E_c} \left[\sigma_{\theta\theta}^{(c)2} + 2(1+\nu_c) \tau_{rz}^{(c)2} \right] r \, dr \, dz + \pi \int_0^L \int_{r_{ec}}^{r_e} \left[\frac{\sigma_{\theta\theta}^{(2)2}}{E_{2t}} + \frac{\sigma_{zz}^{(2)2}}{E_{2l}} - \frac{2\nu_{tl2}}{E_{2t}} \sigma_{zz}^{(2)} \sigma_{\theta\theta}^{(2)} + \frac{1}{G_2} \tau_{rz}^{(2)2} \right] r \, dr \, dz. \quad (16)$$

We replace the expressions of stresses and obtain, after integration over the radius r, the following potential energy expression:

$$\xi_p = \pi \int_0^L \left[A\sigma_{zz}^{(1)2} + B\sigma_{zz}^{(1)} \frac{d^2\sigma_{zz}^{(1)}}{dz^2} + C\left(\frac{d\sigma_{zz}^{(1)}}{dz} \right)^2 + D\sigma_{zz}^{(l)} + E\left(\frac{d^2\sigma_{zz}^{(1)}}{dz^2} \right)^2 + F\frac{d^2\sigma_{zz}^{(1)}}{dz^2} + K \right] dz, \quad (17)$$

where A, B, C, D, E, F and K are constants depending on the load and on the dimensional and mechanical specifications of the two tubes and adhesive.

By carrying out a variational calculus with this last expression of energy and using the boundary conditions in $z = 0$ and $z = L$, we find that the energy is minimal when $\sigma_{zz}^{(1)}$ is the solution of the following differential equation:

$$E\frac{d^4\sigma_{zz}^{(1)}}{dz^4} + (B - C)\frac{d^2\sigma_{zz}^{(1)}}{dz^2} + A\sigma_{zz}^{(1)} + \frac{D}{2} = 0. \quad (18)$$

3. Model application

The application will be presented in the following way: we use the configuration presented in Table 1 and some figures presenting the distribution of stresses and the influence of various parameters affecting the intensity and the distribution of the stress field. This analysis will be reduced to the study of the influence of adhesive thickness, the length of adhesive joint, the Young's modulus of the adhesive and the relative rigidity $E2/E1$.

Fig. 3 gives the force definition, (19), and the radius for which we made the analysis.

$$\pi\left(r_{ic}^2 - r_i^2\right) f = \pi\left(r_e^2 - r_{ec}^2\right) q = F \Rightarrow f = \frac{F}{\pi\left(r_{ic}^2 - r_i^2\right)}. \quad (19)$$

Fig. 4 shows the distributions of stresses in the adhesive for the configuration analysed. We note that the orthoradial stress is more significant than the shear stress.

After studying the influence of the geometrical parameters, we notice that for joints presenting a relatively short covering length, the shear stress adopts a parabolic profile with a maximum in the middle of the adhesive cover. This remark is also made by Shi and Cheng [11], but differs from the distributions of Lubkin [17] and Adams [10], which show two peaks on the free edges; however, it is not validated.

Fig. 5 shows that the covering length has a significant effect on the distribution of shear and orthoradial stresses. We notice that there is an optimal length beyond which the maximum constraints do not change. Moreover, as the covering length increases, we observe:

- compression of shear stress in the middle of the joint and

Table 1
Parameters of the assembly

Tube 1	Adhesive	Tube 2	r_i (mm)	r_{ic} (mm)	r_{ec} (mm)	r_e (mm)	L (mm)	f (MPa)
Aluminium AU 4G $E = 75\,000$ MPa $G = 28\,846$ MPa $\upsilon = 0.3$	Araldite AV 119 $E_c = 2700$ MPa $G_c = 1000$ MPa $\upsilon = 0.35$	Aluminium AU 4G $E = 75\,000$ MPa $G = 28\,846$ MPa $\upsilon = 0.3$	10	11	11.1	12.1	50	1000

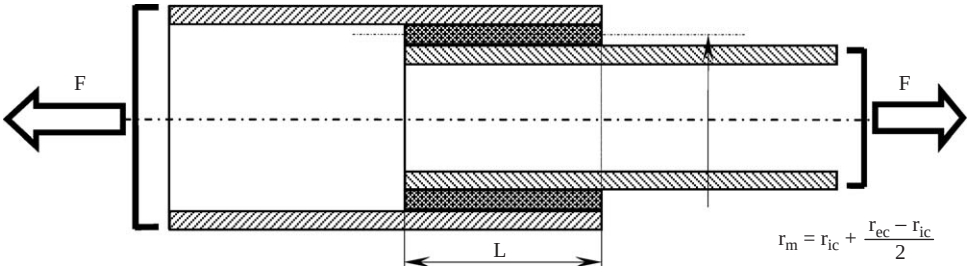

Fig. 3. Definition of the tensile force.

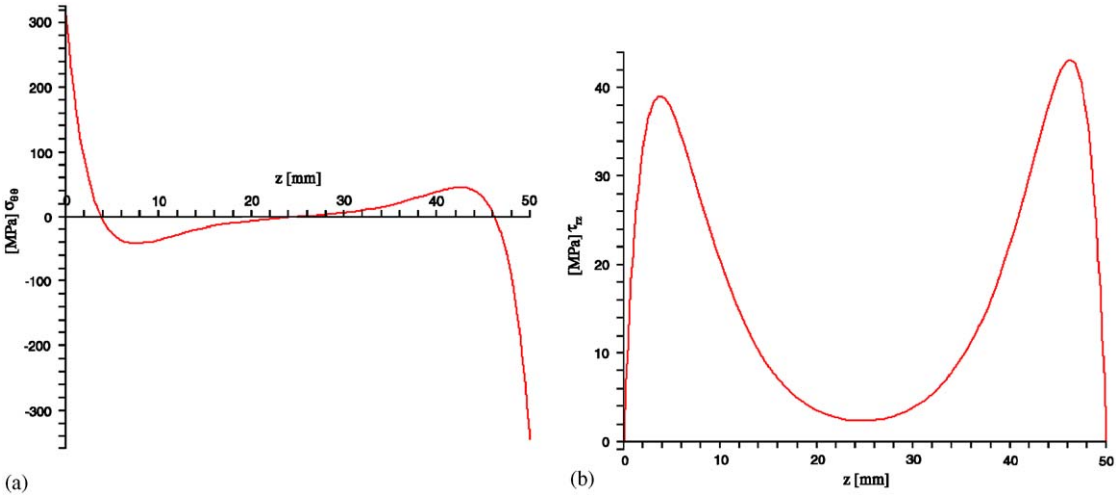

Fig. 4. Stress distribution in the adhesive: (a) orthoradial stress ($\sigma_{\theta\theta}$); (b) shear stress (τ_{rz}).

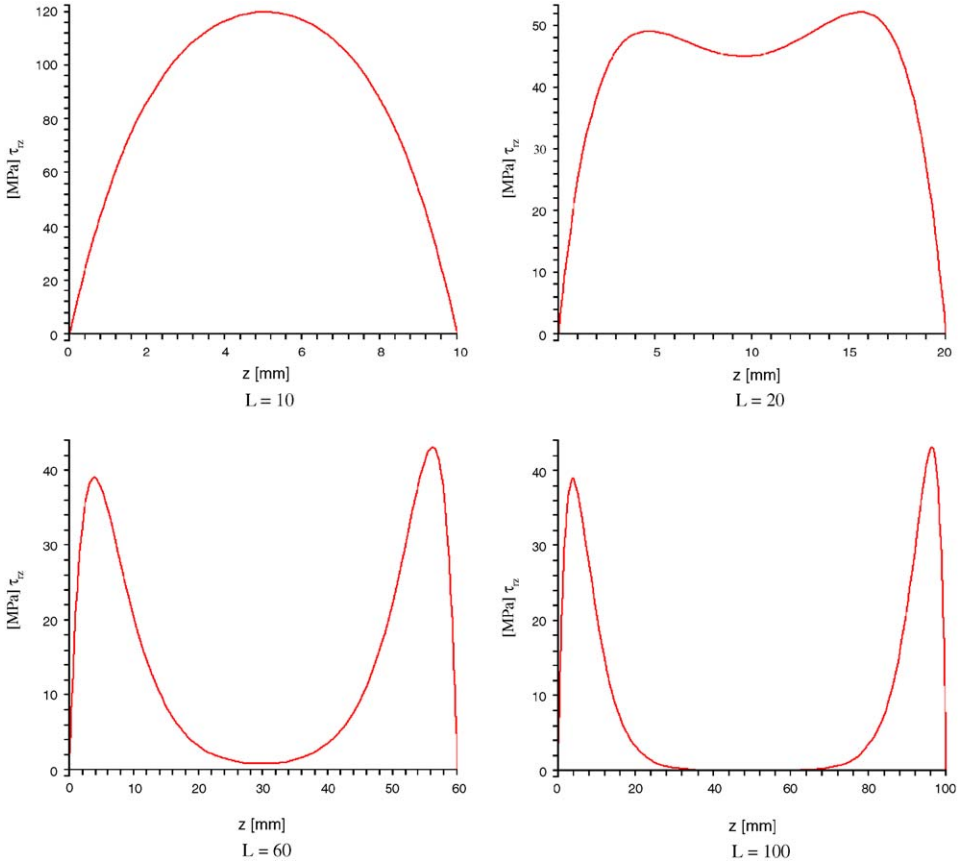

Fig. 5. Variation of shear stress (τ_{rz}) with covering length.

- displacement of the peaks of stress towards the free edges.

Fig. 6 presents the influence of the Young's modulus of the adhesive on the shear stress in the adhesive. We see that the maximum peaks are more significant if the elastic modulus is larger.

The influence of the relative rigidity between two tubes is illustrated in Fig. 7. We observe that the maximum peaks on the two edges are no longer equal if ratio $E2/E1$ is different from 1.

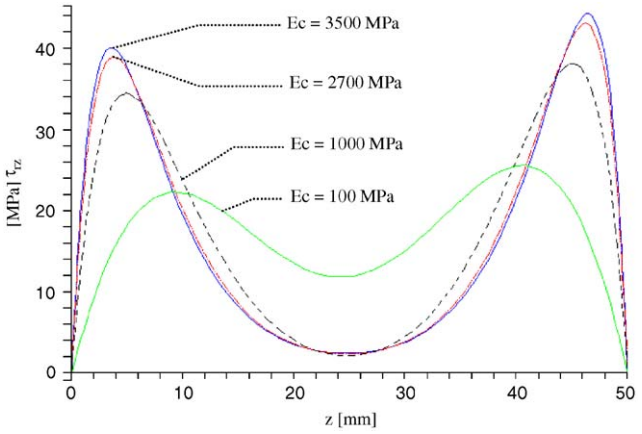

Fig. 6. Variation of shear stress (τ_{rz}) with Young's modulus of adhesive.

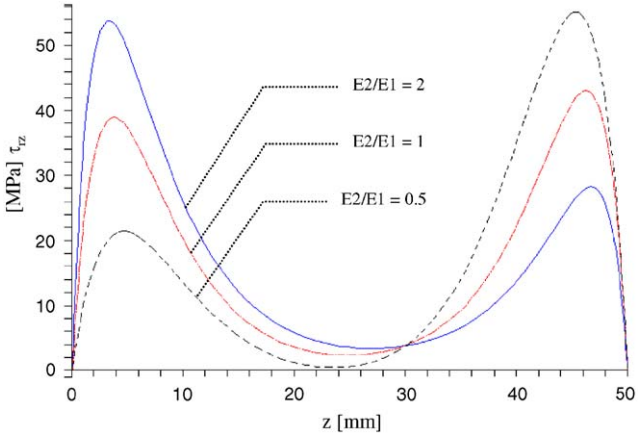

Fig. 7. Variation of shear stress (τ_{rz}) with relative rigidity.

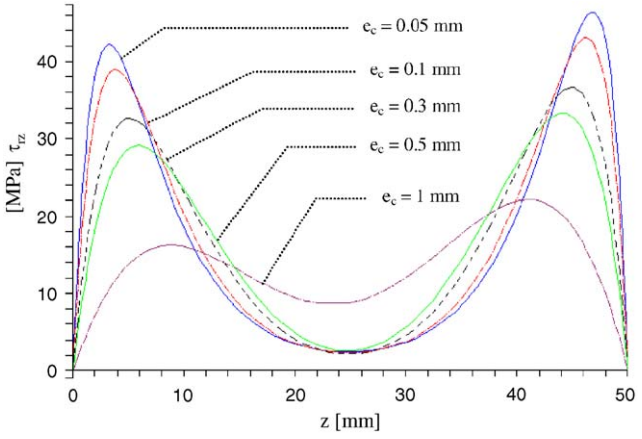

Fig. 8. Variation of shear stress (τ_{rz}) with adhesive thickness.

The influence of the adhesive thickness variation on the distribution and intensity of orthoradial and shear stresses is shown in Figs. 8 and 9. We notice that, when the thickness of the adhesive increases, the values of the two components decrease on the free edges and the distribution becomes more uniform.

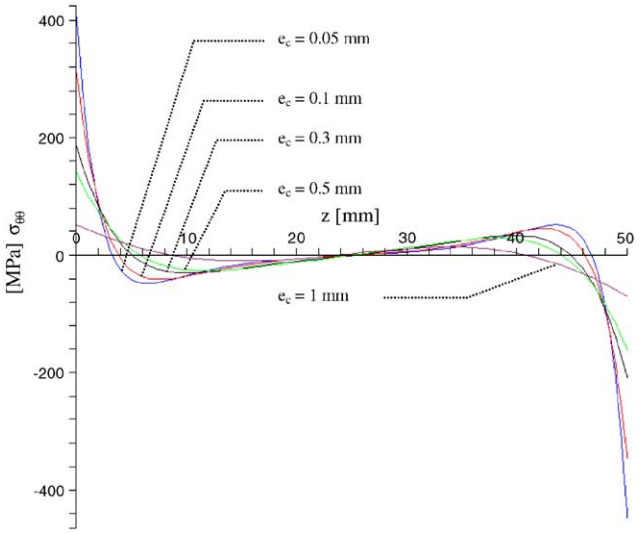

Fig. 9. Variation of orthoradial stress ($\sigma_{\theta\theta}$) with adhesive thickness.

Summary

A simple analytical model for predicting the distribution and intensity of stresses in the adhesive joint has been developed. The model is based on a variational method applied to the potential energy in the assembly. The model can be used to predict the stress field in the assembly or the influence of some geometrical or material parameters on the stress field.

We observe that when the thickness of the adhesive is increased, the values of the stresses in the adhesive decrease on the free edges and the distribution becomes more uniform.

References

[1] Volkersen O. Die Nietkraftverteilung in Zugbeanspruchten Nietverbindungen mit Konstanten Laschenquerschnitten. Luftfahrtforschung 1938;15:41–7.
[2] Tsai MY, Oplinger DW, Morton J. Improved theoretical solutions for adhesive lap joints. Int J Solid Struct 1998;35(12):1163–85.
[3] Li G, Lee-Sullivan P. Finite element and experimental studies on single-lap balanced joints in tension. Int J Adhesion Adhes 2001;21:211–20.
[4] Chalkley P, Rose F. Stress analysis of double-lap bonded joints using a variational method. Int J Adhesion Adhes 2001;21:241–7.
[5] Conçavales JPM, de Moura MFSF, de Castro PMST. A three-dimensional finite element model for stress analysis of adhesive joints. Int J Adhesion Adhes 2002;22:357–65.
[6] Mortensen F, Thomsen OT. Coupling effects in adhesive bonded joints. Compos Struct 2002;56:165–74.
[7] Mortensen F, Thomsen OT. Analysis of adhesive bonded joints: a unified approach. Compos Sci Technol 2002;62:1011–31.
[8] Xiao X, Foss PH, Schroeder JA. Stiffness prediction of the double lap shear joint. Part 1: analytical solution. Int J Adhesion Adhes 2004;24:229–37.
[9] Xiao X, Foss PH, Schroeder JA. Stiffness prediction of the double lap shear joint Part 2: analytical solution. Int J Adhesion Adhes 2004;24:239–46.

[10] Adams RD, Peppiatt N. Stress analysis of adhesive bonded tubular lap joints. J Adhesion 1977;9:1–18.
[11] Shi YP, Cheng S. Analysis of adhesive-bonded cylindrical lap joints subjected to axial load. J Eng Mech 1993;119:584–602.
[12] Serrano E. Glued-in rods for timber structure—a 3D model and finite element parameter studies. Int J Adhesion Adhes 2001;21:115–27.
[13] Çolak A. Parametric study of factors affecting the pull-out strength of steel rods bonded into precast concrete panels. Int J Adhesion Adhes 2001;21:487–93.
[14] Bainbridge R, Mettem C, Harvey K, Ansell M. Bonded-in rod connections for timber structures—development of design methods and test observations. Int J Adhesion Adhes 2002;22:47–59.
[15] Kawamura H, Sawa T, Yoneno M, Nakamura T. Effect of fitted position on stress distribution and strength of a bonded shrink fitted joint subjected to torsion. Int J Adhesion Adhes 2003;23: 131–40.
[16] Vaziri A, Nayeb-Hashemi H. Dynamic response of tubular joints with an annular void subjected to a harmonic axial load. Int J Adhesion Adhes 2002;22:367–73.
[17] Lubkin L, Reissner E. Stress distribution and design data for adhesive lap joints between circular tubes, Trans of ASME. J Appl Mech 1956;78:1213–21.
[18] Alwar RS, Nagaraja YR. Viscoelastic analysis of an adhesive tubular joint. J Adhesion 1976;8:76–92.